*Clays and Clay Minerals*, Vol. 58, No. 4, 573–584, 2010.

# ORIGIN AND DEPOSITIONAL ENVIRONMENT OF PALYGORSKITE AND SEPIOLITE FROM THE YPRESIAN PHOSPHATIC SERIES, SOUTHWESTERN TUNISIA

A. Tlili*, M. Felhi, and M. Montacer

Earth Sciences Department, Sciences Faculty of Sfax, Route de Soukra, Km 3.5, BP 802, 3038 Sfax, Tunisia

**Abstract**—The Ypresian phosphatic series of the Gafsa-Metlaoui basin, southwestern Tunisia, is represented by an alternation of phosphatic levels and interbedded facies, which are composed of marly clay and silica-rich rocks. The present work aimed to clarify the genesis of palygorskite and sepiolite of the interbedded facies and to understand the depositional environment of the phosphatic series. The interbedded facies of the Stah and Jellabia mines were investigated using X-ray diffraction (XRD), scanning electron microscopy (SEM), and Energy Dispersive X-ray microanalysis (EDX) of individual constituents and their aggregates. The data obtained indicate that samples are made up of francolite, calcite, dolomite, quartz, feldspars, and clay minerals; the latter consist of palygorskite-sepiolite minerals associated with smectite. Observations by SEM revealed the occurrence of palygorskite and sepiolite as fine and filamentous fibers with thread-like facies and coating dolomite, calcite, and a marly matrix. Such features can be considered as textural evidence of authigenic palygorskite-sepiolite. At the bottom of the Stah section, SEM observations revealed that the fine fibers are more abundant within silica-rich rocks. Silica is commonly available due to bacterial activity saturating its environment with the silicic acid required for the formation of palygorskite-sepiolite. In the interbedded facies of the Jellabia section, the moderate fibrous clay content and the presence of well crystallized dolomite revealed that the shallow-marine water was characterized by high-Mg and low-Si activities.

**Key Words**—Alkalinity, Authigenesis, Bacterial Activity, Sepiolite, Palygorskite.

## INTRODUCTION

Palygorskite and sepiolite are characterized by similar physical proprieties but their bulk chemical compositions are different (García-Romero *et al.*, 2007; Pluth *et al.*, 1997). Several studies have shown that sepiolite is characterized by a large Mg content. Palygorskite is distinguished by the substitution of some Mg by Fe and/or Al (Jones and Galán, 1988; Frost *et al.*, 2001; Krekeler *et al.*, 2008). The structure of sepiolite and palygorskite consists of channels that lie between the backs of opposing 2:1 layers. Each channel contains zeolitic water, ordered and linked to octahedral Mg.

Multiple modes of occurrence of palygorskite and/or sepiolite have been established in the last few decades. Several studies have indicated that fibrous clays precipitate from natural or synthetic solutions (Jones and Galán, 1988; Krekeler *et al.*, 2004; García-Romero *et al.*, 2007; Birsoy, 2002); weathering of volcanic ash; diagenetic transformation of smectitic clays, Mg-carbonate, and serpentines (Weaver and Beck, 1977; Chahi *et al.*, 1993; Yalcin and Bozkaya, 1995); and neo-formation (Millot, 1970; Singer and Norrish, 1974). Palygorskite and sepiolite have been found in marine, lacustrine environments, in continental soils, and in association with igneous rocks (Jones and Galán, 1988), and they are probably associated with phosphate, carbonate, and silica sedimentary deposits (Isphording, 1973).

The phosphatic series in the Gafsa-Metlaoui basin (southwestern Tunisia) consists mainly of three lithofacies: the phosphatic levels, the marly clays, and the limestone deposits (Visse, 1952; Burollet, 1956; Sassi, 1974; Belayouni, 1983; Chaâbani, 1995; Henchiri and Slim-Shimi, 2006; Henchiri, 2007; Felhi *et al.*, 2008b, Felhi, 2010). Several previous studies concentrated on marine sedimentary phosphatic layers due to their special economic interest and showed that palygorskite-sepiolite minerals are present in the regional phosphatic series, which are actually mined in many areas of the Gafsa-Metlaoui basin (Visse, 1952; Burollet, 1956; Sassi, 1974). Other mineralogical and geochemical studies have revealed that palygorskite-sepiolite minerals associated with smectite occurred mainly within the Ypresian series (Chaâbani, 1995; Jamoussi *et al.*, 2003b). Supplementary investigations demonstrated that cherty levels, associated with the Ypresian phosphatic series, become more and more abundant in the western part of the Gafsa-Metlaoui basin (Sassi, 1974). Silica-rich deposits, characterized by the neoformation of palygorskite, are identified in other early Eocene deep-water sediments such as the Western Central Atlantic and Gulf of Guinea (Pletsch, 2001). The regional study by Zaaboub *et al.* (2005) concerning the origin of fibrous clays in Tunisian Paleogene

* E-mail address of corresponding author:
alitlili@yahoo.fr
DOI: 10.1346/CCMN.2010.0580411

continental deposits provided geochemical and mineralogical evidence of the neo-formation of palygorskite-sepiolite. Felhi *et al.* (2008b) demonstrated that the lower part of the Ypresian marine phosphatic series (Stah section) containing a cherty level are characterized by relatively large amounts of palygorskite-sepiolite.

The aim of the present work was to investigate the co-occurrence of palygorskite and sepiolite minerals contained in the phosphatic series for which the mineralogy and textural properties are relatively unknown. The co-occurrence of the two minerals presents an interesting opportunity to understand better the genesis of palygorskite-sepiolite and to elucidate the depositional environment.

## GEOLOGIC SETTING AND LITHOLOGICAL DESCRIPTION

The Gafsa-Metlaoui basin is located in the south-western part of Tunisia, between 34º and 35ºN latitude and 8º and 10ºE longitude (Figure 1). Detailed structural and sedimentological characteristics of the outcropping deposits in this basin have been described by several authors (Sassi, 1974; Chaâbani, 1995; Henchiri and Slim-Shimi, 2006). As data for the organic matter contained in the phosphatic series were provided by Belayouni (1983), an overview of the Ypresian lithofacies in the Gafsa-Metlaoui basin is given here.

According to Visse (1952) and Sassi (1974), the Ypresian phosphatic series, which consists of nine phosphatic layers interbedded with marly clays and metric cherty levels, are also interpreted as marine sedimentary deposits with a cyclic character. The marine origin is, however, confirmed by the organic matter-based studies of Belayouni (1983), and Felhi *et al.* (2008b).

The paleogeographic map of Tunisia during the Ypresian period, established by Castany (1951) and modified by Burollet (1956), Sassi (1974), Burollet and Oudin (1980), and Chaâbani (1995), shows that the Gafsa-Metlaoui basin is situated between three emerged zones, *i.e*. the so-called Kasserine island in the north, the so-called Djeffara island in the south, and the so-called Algerian promontory in the northwest. This basin is, however, connected to the Tethys Ocean *via* the so-called Shemsi sill, which permitted the entry of fresh water from the open sea during the upwelling (Figure 1). The upwelling supplied this restricted basin with nutrient-rich water which increased the primary production considerably. The productivity of siliceous shells in the photic water layer and their dissolution in seawater saturated the depositional environment with silicic acid which is required for the authigenesis of palygorskite and sepiolite.

In order to study the depositional environment and the mode of occurrence of palygorskite-sepiolite miner-

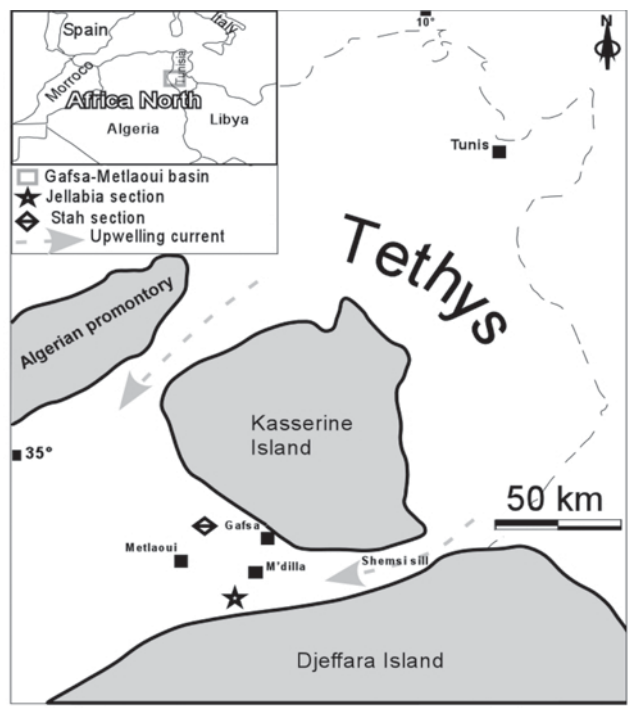


Figure 1. Paleogeographic map of Tunisia during the Ypresian period, showing the position of Gafsa Metlaoui basin (Burrolet, 1956; Sassi, 1974; Burollet and Oudin, 1980; Chaâbani, 1995). The locations of the Ypresian sections studied are indicated by an asterisk. The Jellabia section, located at the border of the basin with Djeffara Island, corresponds to shallow sea water. The Stah section, located near the central part of the basin, corresponds to deep sea water.

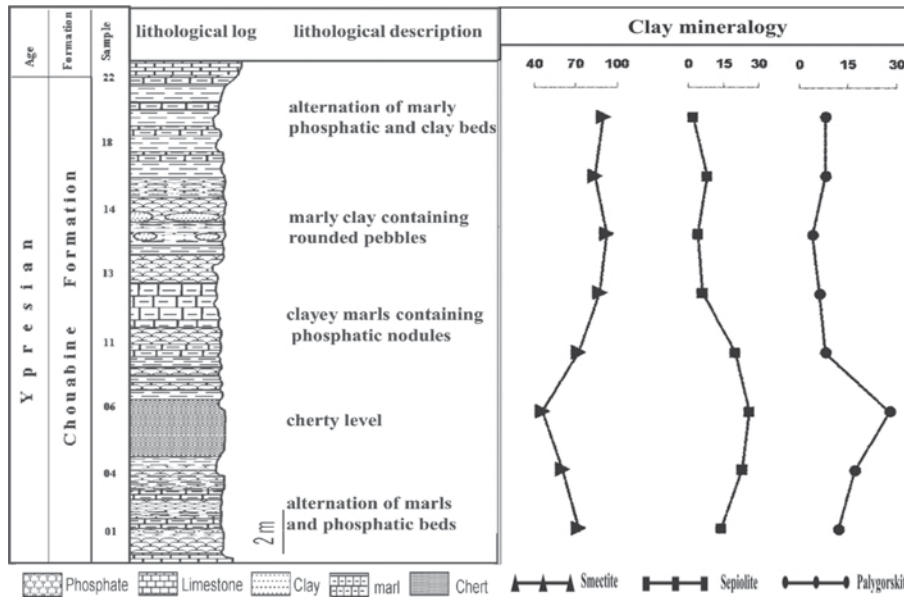


Figure 2. Lithological description along the Ypresian phosphatic series and the trends of the clay contents (Stah section).

als that are correlated to phosphatic or silica-rich rocks in the Gafsa-Metlaoui basin, two Ypresian-age sections were sampled from the Stah and the Jellabia mines, located in the central part and in the eastern limit of the basin, respectively (Figure 1). Both sections are limited at the bottom by the gypsum deposits of the Selja Formation and at the top by the massive limestones of the Kef Eddour Formation as defined by several authors (*e.g.* Burollet, 1956; Sassi, 1974; Belayouni, 1983; Zargouni, 1985; Chaâbani, 1995). Lithologically, both sections are mainly represented by an alternation of marly clays and phosphatic levels. While the lower part of the Stah section is distinguished by the presence of a 3.5 m thick cherty level (Figure 2) (Felhi *et al.*, 2008b), the upper part of the Jellabia section is marked by the existence of siliceous phosphatic beds containing arenite-sized quartz grains with bioturbation and two levels of oyster fragments (Figure 3).

## MATERIAL AND METHODS

A total of 18 sediment specimens were sampled from the two mines. Eight specimens were sampled from the marly clays and cherty level of the Stah section and ten

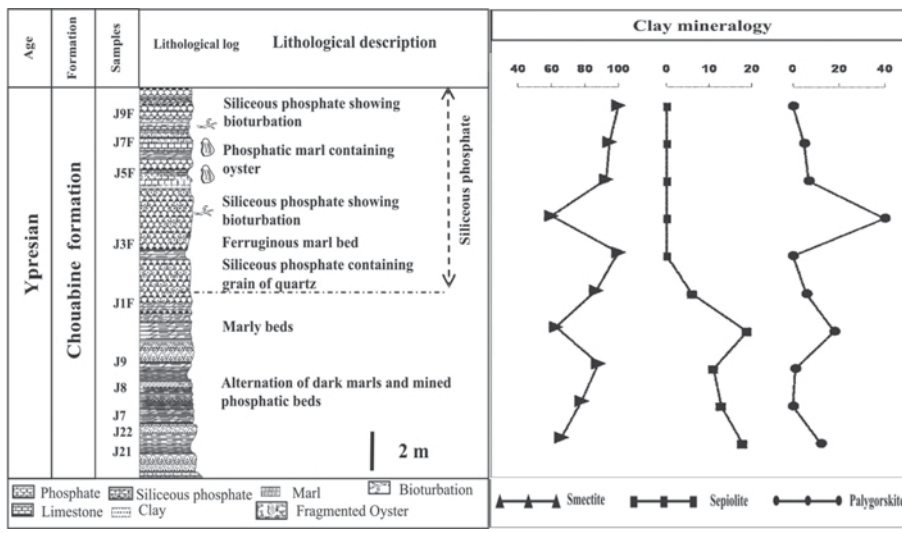


Figure 3. Lithological description along the Ypresian phosphatic series and the trends of the clay contents (Jellabia section).

specimens were sampled from the Jellabia marly clays. The Stah specimens are characterized by a greenish beige color. The Jellabia specimens are distinguished by a black color in the lower part, which may indicate that they are relatively rich in organic matter. They become red-brown in the upper part, which may indicate that they are rich in Fe.

The clay fraction (<2 μm particles) was separated from those samples by sedimentation and centrifugation (Brindley and Brown, 1980; Felhi *et al.*, 2008a). X-ray diffraction patterns of the finely crushed bulk rocks and of the three oriented samples of the <2 μm fraction (air-dried, ethylene glycol-saturated, and heated at 550ºC) were used in order to determine the whole-rock mineralogy and clay-mineral associations, respectively. The percentage of each clay mineral was determined from the peak area of the 001 reflection in the oriented sample of the <2 μm clay fraction and the ethylene glycol-saturated sample (Schultz, 1964; Fakhfakh *et al*., 2007). For bulk rock, all clay-mineral content was determined from the surface area of the peak at 4.45 Å, where the percentages of francolite, calcite, dolomite, feldspars, and quartz were estimated from surface areas of their strong reflections (Felhi *et al*., 2008b). The XRD measurements were carried out in the Laboratoire des Ressources Minérales et Environnement of the Faculty of Sciences of Tunis with an X'pert HighScore plus PANalytical diffractometer, equipped with a CoKα radiation source and operated at 40 kV/40 mA. All XRD data were collected under the same experimental conditions: an angular range of $3^\circ \leqslant 2\theta \leqslant 45^\circ$, a step size of 0.017º2θ, and a counting time of 10 s/step. Based on the clay and bulk-rock mineralogy, SEM observations were undertaken on selected samples of interbedded facies to emphasize the morphological features of the palygorkite-sepiolite minerals and their textural relations to the other associated minerals. The specimens were mounted on a Scanning Electron Microscope (SEM) stub, coated with a thin layer of gold, and examined using a Philips® 30 Analytical Scanning Electron Microscope equipped with an EDX system for the characterization of the elemental composition of crystals. *n*-Alkane (m/z = 57) distributions of saturated hydrocarbons associated with the finer fraction were accomplished using Gas Chromatography Mass Spectrometry (GC-MS) to determine the origin of organic matter associated with the clay fractions. The description of this technique is summarized in the studies of Arfaoui and Montacer (2007) and Felhi *et al.* (2008b).

## RESULTS

### *XRD data*

The XRD patterns of three bulk-rock samples (J21, J8, and J3F), collected from the Jellabia section, revealed that they are composed mainly of francolite, calcite, dolomite, quartz, feldspars, and clay minerals (smectite, palygorskite, and sepiolite). The strong reflections of these minerals appear at 2.79 Å, 3.03 Å, 2.89 Å, 3.34 Å, 3.19 Å, and 4.45 Å, respectively (Figure 4: J21, J8, and J3F). The XRD patterns of the <2 μm fraction (untreated, glycolated, and heated at 550ºC) of the samples J21, J8, and J3F (Figure 5) revealed that the clay fraction consists of smectite, sepiolite, and playgorskite. Their respective 001 reflections are ~15 Å, 12.04 Å, and 10.5 Å (Figure 5). The characteristic peak of smectite in each air-dried sample expanded to ~17.6 Å after saturation with ethylene glycol and collapsed to 10 Å when heated at 550ºC.

Smectite, playgorskite, and sepiolite constitute the clay fractions of samples selected from the Jellabia section. The trends of the clay content in these samples indicate that the palygorskite-sepiolite minerals are relatively more concentrated in the lower part of the section (Figure 3). However, the clay mineral assemblages are represented only by palygorskite and smectite in the upper part (Figure 3). The 001 characteristic peak of sepiolite is absent from the XRD patterns of sample J3F (Figure 5). In the bulk rock, the clay fractions are probably mixed with francolite, calcite, dolomite, quartz, and feldspars. The percentage of dolomite and calcite varies from 6 to 82% and from 2 to 26%, respectively. However, clay minerals are more abundant

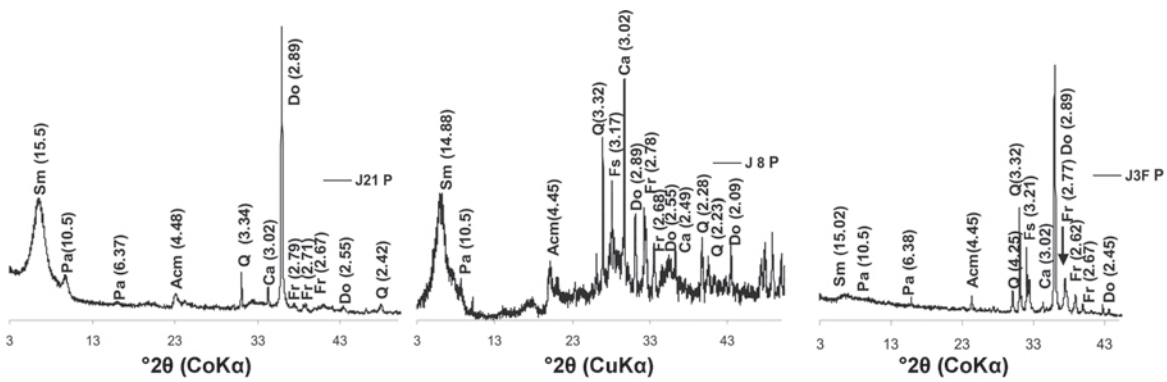


Figure 4. XRD patterns (CoKα radiation) of the J21, J8, and J3F bulk-rock samples (Sm: smectite; Acm: all clay minerals; Fr: francolite; Fs: feldspar; Ca: calcite; Do: dolomite; Q: quartz; P: powder).

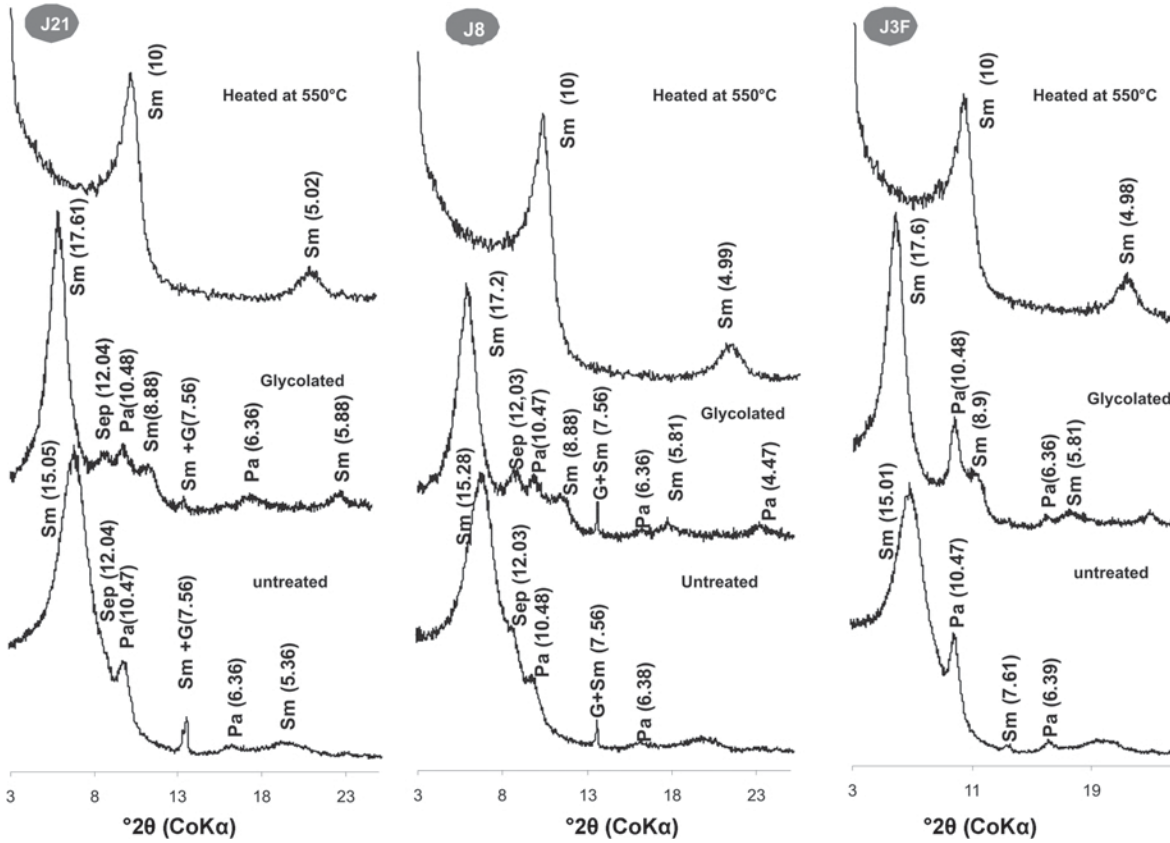


Figure 5. XRD patterns (CoKα radiation) of three oriented clay fractions of the samples J21, J8, and J3F (Sm: smectite; Sep: sepiolite; Pa: palygorskite, G: gypsum).

in samples J21, J22, J8, and J9F. The greatest percentages of quartz are found in samples J3F and J9F (26 and 32%, respectively), collected from the upper part of the Jellabia section (Table 1).

The mineralogical content of the clay fraction of the Stah section was given in a previous study by Felhi *et al.* (2008b). Notice, however, that the amounts of palygorskite and sepiolite present similar trends, which vary in inverse proportion to that of smectite. In addition, the palygorskite-sepiolite minerals are clearly more concentrated in the cherty level, where they reach roughly 50% in sample SN6. In contrast, smectite becomes the most abundant clay mineral below and above this level in the section (Figure 2).

*SEM investigations*

The SEM images of the samples selected from the Stah section revealed that the marly clays display a fibrous texture characterized by the abundance of fine fibers coating rhombohedral calcite (Figure 6*A*), which

Table 1. Bulk-rock mineralogy (%) of samples from Jellabia.

| Sample | Calcite | Dolomite | All clay minerals | Francolite | Feldspars | Quartz |
|---|---|---|---|---|---|---|
| J21 | 4 | 67 | 10 | 4 | 7 | 8 |
| J22 | 5 | 67 | 8 | 8 | 5 | 7 |
| J7 | 10 | 36 | 28 | 17 | 1 | 8 |
| J8 | 26 | 18 | 18 | 18 | 3 | 17 |
| J9 | 7 | 74 | 5 | 5 | 4 | 5 |
| J1F | 3 | 82 | 6 | 1 | 5 | 3 |
| J3F | 4 | 48 | 5 | 9 | 8 | 26 |
| J5F | 2 | 81 | 6 | 3 | 5 | 3 |
| J7F | 2 | 68 | 7 | 5 | 7 | 11 |
| J9F | 2 | 6 | 53 | 2 | 5 | 32 |

was confirmed by the dominance of Ca in the EDX analysis of these rhombs (Figure 6*a*). Palygorskite and sepiolite minerals grew in the pore spaces and on the surface of marly clays, where they formed a fibrous mat. These fibers, which are more abundant and which do not exceed 1 μm in length in sample SN6 (Figure 6*C*), are very fine in sample SN14, where they coat the marly matrix (Figure 6*E*, 6*F*). At the top of the section, the palygorskite-sepiolite minerals are elongated and tangled. The length of the filamentous fibers often exceeds 5 μm (Figure 6*H*) and their EDX analyses show the presence of Ca, Fe, Mg, Si, and Al (Figure 6*h*).

Micrographs of the Jellabia selected samples revealed that the dolomite rhombohedra are disseminated within the microgranular facies (Figure 7*A*, 7*B*). These dolomite rhombs are well crystallized, showing developed crystal faces, particularly in the lower part of the section. They are relatively more abundant in samples J21 and J22 compared to samples J7 and J8. The rhombohedral forms of samples J7 and J8 are slightly weathered in contrast to those of samples J3F and J7F, sampled from the top, in which the crystal faces are completely altered. As indicated by XRD analysis of the clay fraction, J3F is characterized by a large amount of palygorskite (Figure 7*H*). On the other hand, SEM images show that samples J7 and J8 are distinguished by thread-like facies characterizing the fibrous clays. This is in accord with the large amount of palygorskite-sepiolite computed from the XRD patterns (Figure 5). In the Jellabia section, an abundance of crystallized dolomite was observed in the marine sedimentary phosphatic facies at the base, whereas weathered dolomite was observed in the siliceous phosphatic facies at the top.

The texture of palygorskite-sepiolite minerals may be related to the mineralogical association of the bulk rocks, which characterize the depositional environment. The fiber and filamentous textures were mostly observed in the Stah samples, where silica-rich rock samples show only a fibrous texture of palygorskite-sepiolite roughly in the same proportion, as revealed by XRD analysis (Figure 3). The thread-like facies and fine fiber texture of palygorskite-sepiolite observed in the Jellabia samples are mainly associated with the dolomite (Figure 7*F*, 7*H*). Distinguishing between fibrous palygorskite and sepiolite from SEM observations is difficult because of the mixing of their fine fibers, although sample J3F displays thread-like palygorskite associated with faintly weathered dolomite. A silica-rich environment apparently favors the genesis of palygorskite-sepiolite with a fibrous texture. A dolomite-rich environment, however, favors the formation of the thread-like facies, though the thin fiber texture was also observed.

### *n-alkane distribution along the Jellabia section*

Experimental measurement of the *n*-alkane (m/z = 57) distribution of saturated hydrocarbons of three samples J21, J8, and J1F that belong to the lower and upper parts of the Jellabia section, respectively (Figure 8), revealed that the fragmentogram of the J21 sample has a bimodal distribution, $n$-$C_{16}$–$n$-$C_{19}$ and $n$-$C_{20}$–$n$-$C_{25}$, indicating that organic matter has both a phytoplanktonic and bacterial origin. For the J8 and J1F samples, the *n*-alkanes (m/z = 57) range from $n$-$C_{16}$–$n$-$C_{22}$ and $n$-$C_{17}$–$n$-$C_{22}$, respectively, which shows that the organic matter has a phytoplanktonic origin (*e.g.* Disnar *et al.*, 1996), from the middle to the top of this section.

## DISCUSSION

The main sedimentary marine phosphatic series was deposited during the Ypresian period in the Gafsa-Metlaoui basin (Sassi, 1974; Belayouni, 1983; Chaâbani, 1995). Marly clays and silica-rich rock layers represent the main facies of the interbedded levels of the Ypresian phosphatic series, whereas smectite and palygorskite-sepiolite constitute the clay fraction. The occurrence of these minerals requires a Mg-rich environment, which agrees with the abundance of dolomite revealed by SEM investigation. The occurrence of palygorskite during a contemporaneous period in northwest Africa (Morocco) was also related to the sufficient Mg concentrations in the marine water (Daoudi, 2004). The absence of such clay minerals (smectite, palygorskite, and sepiolite) in the phosphorite of Egypt, however, may be related to low Mg in sea water during the Cretaceous (Baioumy *et al*., 2007).

The trends in variation of these clay mineral assemblages along the two selected sections (Jellabia and Stah) show that palygorskite-sepiolite minerals are more concentrated at the lowermost part, but with variable proportions. The SEM observations of the Jallabia samples show that thin, fibrous, thread-like palygorskite-sepiolite forms as a coating on weathered dolomite (Figure 7). This texture can be considered as an authigenic character of these fibrous minerals, as the occurrence of palygorskite-sepiolite minerals covering dolomite are recognized to be authigenic in origin rather than detrital (*e.g.* Estéoule-Choux, 1984; Daouadi, 2004). Textural evidence of the authigenesis of palygorskite-sepiolite occurs commonly in the Stah samples. The main features observed were the presence of fine clay fibers coating the marly matrix (Figure 6) and the abundance of fibrous mats especially in the cherty level (Figure 6*C*, 6*D*). Those minerals can also be formed by transformation from smectite, as suggested by Singer (1984); but, the assumption that fibrous clays associated with interbedded facies have originated by transformation from smectite is unlikely to be valid due to the significant difference between smectite and palygorskite-sepiolite mineral structures, as reported by Singer (1979) and Chahi (1996), and also due to the small degree of diagenesis of the phosphatic series, which does not exceed early digenesis (Sassi, 1974; Belayouni, 1983). In addition, smectite transformation was not revealed by the SEM investigations in the lower part of

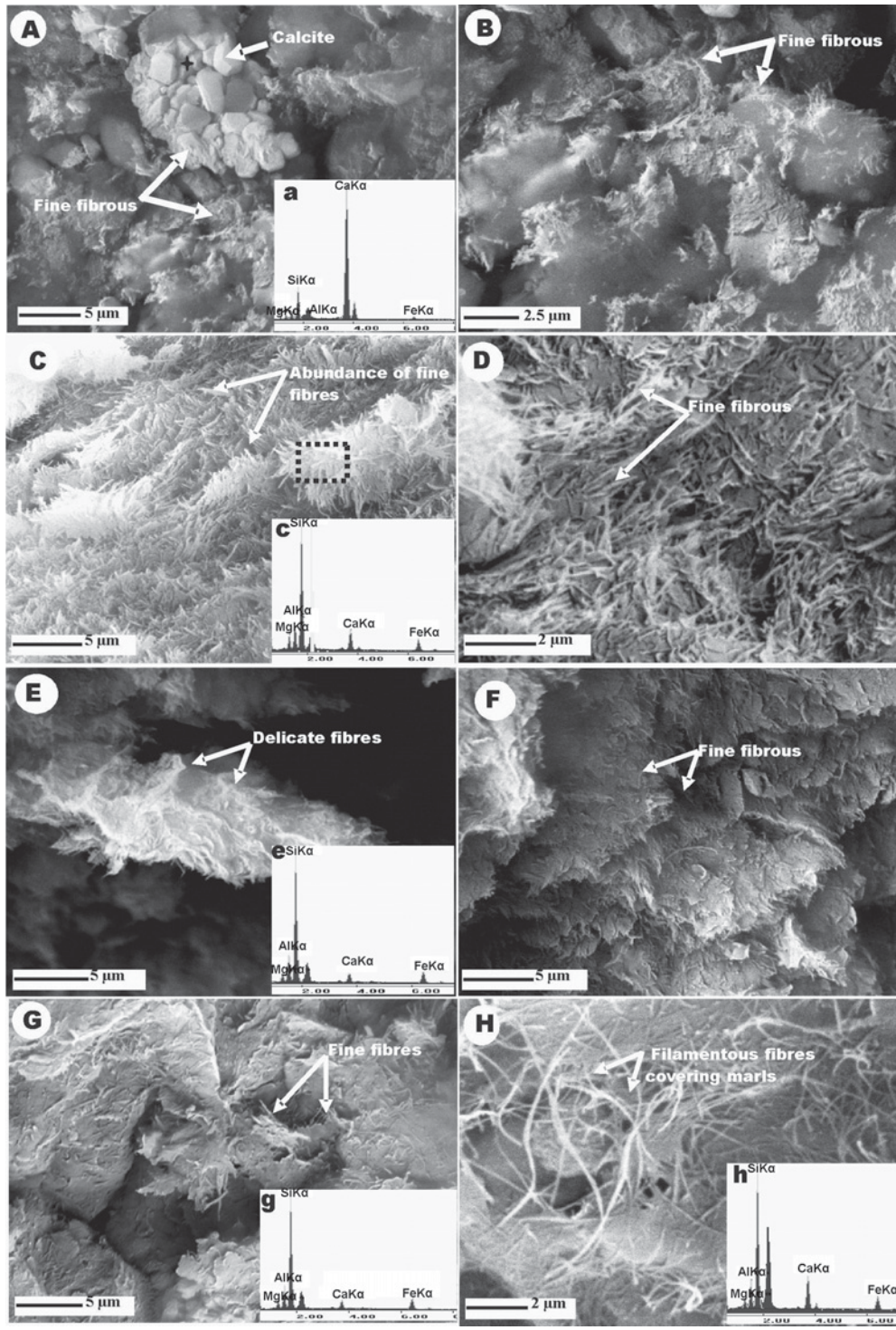


Figure 6. SEM images of selected samples from the Stah section. (*A*) Sample SN4 showing thin fibers coating calcite rhombohedra. (*a*) EDX of calcite rhombohedra reveals the presence of Ca, Mg, Si, and Fe. (*B*) Sample SN4 showing fine fibers coating the matrix. (*C*) Sample SN6 showing an abundance of fiber mats in the sample from cherty level. (*c*) EDX of the fine fibers revealing the presence of Ca, Mg, Si, and Al. (*D*) Sample SN6 showing delicate fibers associated with marls. (*d*) EDX showing the presence of Mg, Si, Al, and Fe. (*E*) Sample SN14 showing palygorskite and sepiolite coating marls. (*e*) EDX showing the large amounts of Si. (*F*) Sample SN14 showing short fibers coating marls. (*G*) Sample SN14 showing fine fibers growing in the pore space. (*g*) EDX showing the presence of Mg, Si, Al, and Fe. (*H*) Sample SN18 showing filamentous fibers. (*h*) EDX showing the presence of Mg, Si, Al, and Fe.

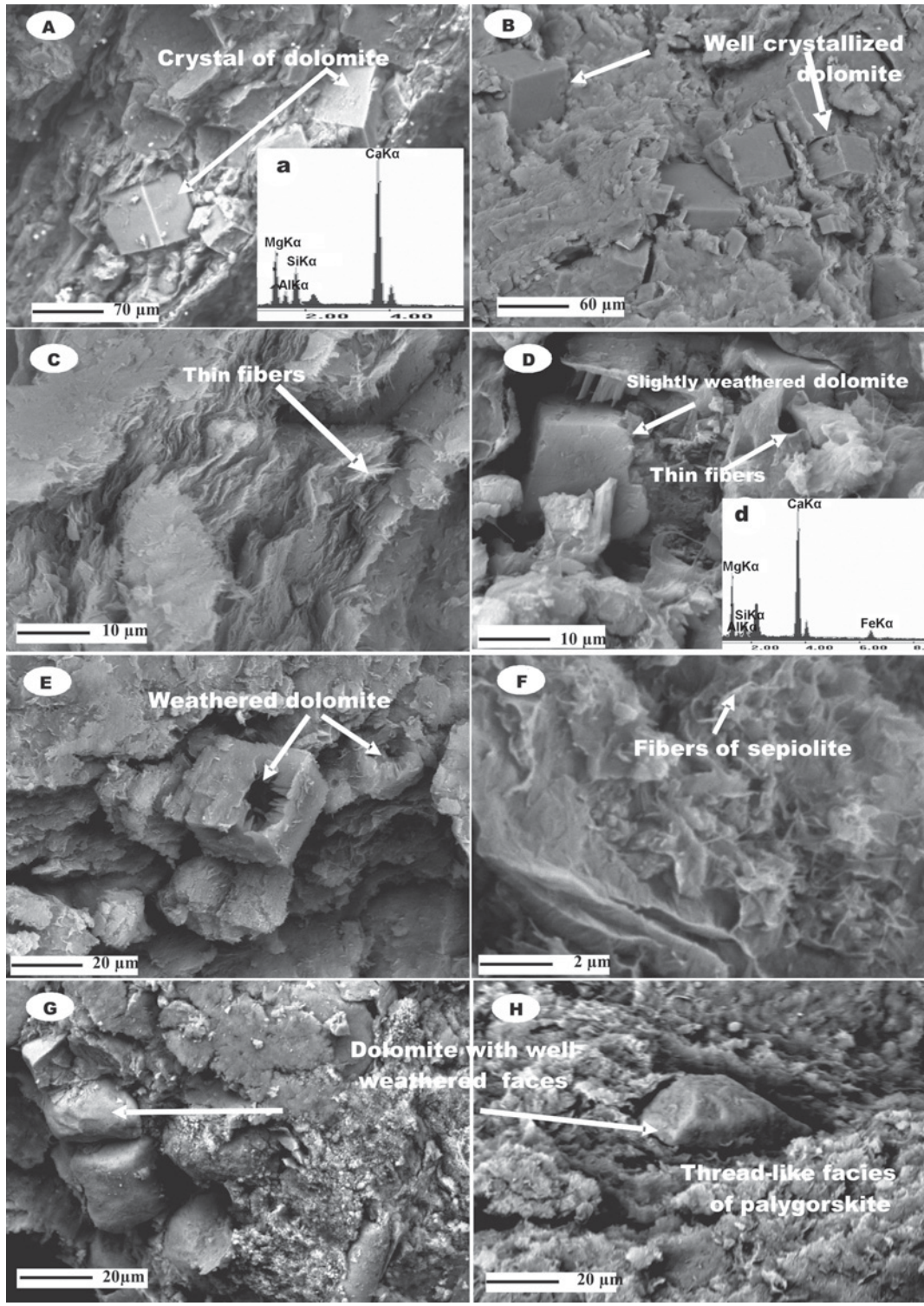


Figure 7. SEM images of selected samples from the Jellabia section. (*A*) Sample J21 showing well developed crystals of dolomite. (*a*) EDX of dolomite rhombohedra reveals the presence of Ca and Mg. (*B*) Sample J22 showing an abundance of well crystallized dolomite disseminated within the clays. (*C*) Sample J22 showing thin fibers. (*D*) Sample J7 showing weathered dolomite covered by thin fibers. (*d*) EDX of dolomite rhombohedra reveals the presence of Ca and Mg. (*E*) Sample J8 showing delicate, short fibers associated with weathered dolomite crystals. (*F*) Sample J8 showing thread-like sepiolite and thin lamellae. (*G*) Sample J7F showing weathered dolomite. (*H*) Sample J3F showing weathered dolomite in thread-like palygorskite.

the Stah or above the cherty bedded unit. The palygorskite-sepiolite minerals probably grew during early diagenesis. The development of fibers on carbonates and silica-rich rocks may indicate that palygorskite-sepiolite crystallize after the formation of calcite, dolomite, and chert.

The significant amount of palygorskite-sepiolite in silica-rich rocks (Figure 3) indicates that some genetic relation may exist between them. According to Lancelet (1973) and Muttoni and Kent (2007), the formation of palygorskite is favored by an absorption of silica from silica-rich rocks. Excess Si during the formation of cherts promotes direct crystallization of palygorskite-sepiolite minerals. A rich silica environment apparently restrained the abundance of fibrous clays. Authigenic playgorskite is also noted in deep-sea chert of early Eocene age from the Western Central Atlantic (Pletsch, 2001). Several studies have reported that the direct crystallization of palygorskite-sepiolite minerals from solution needs specific conditions such as high Mg and Si activities and a small amount of Al under alkaline pH conditions of environmental deposits (Weaver and Beck, 1977; Velde, 1985; Jamoussi *et al.*, 2003a).

The depositional environment of the Ypresian phosphatic series of the Gafsa Metlaoui basin was characterized by the great productivity of siliceous shells and a thick water column, which induced stratified water as reported by Henchiri (2007). The stratification encouraged anoxic conditions at the bottom, where bacteria proliferated from sedimentary organic matter (Figure 9). The increasing productivity of biosiliceous organisms generated biogenic silica, which dissolved at a high degree of alkalinity inducing a silicic acid-saturated environment.

Previous geochemical studies of organic matter in several areas of the basin (Belayouni, 1983) have revealed that the organic matter has bacterial and phytoplanctonic origins, in accord with the data obtained from the *n*-alkane distributions of hydrocarbons saturated in the lowermost part of the Jellabia section, as revealed by GC-MS analysis (Figure 8). In addition, Felhi *et al*. (2008b) indicated that the cherty beds of the Stah section are characterized by bacterial acitivity, inducing silicic-acid availability for palygorskite-sepiolite formation. According to Bidle and Azam (1999), the dissolution of silica in recent marine deposits can be realized at high

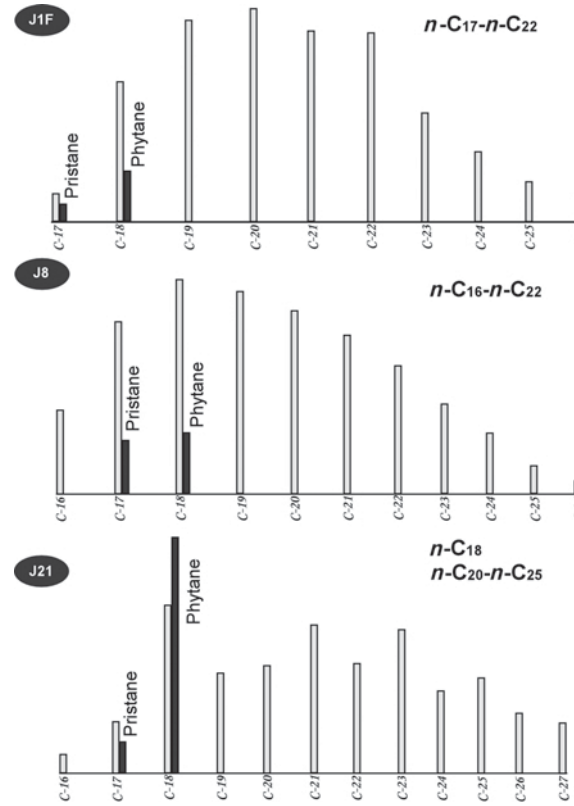


Figure 8. *n*-Alkane (m/z = 57) distribution of saturated hydrocarbons in three Ypresian samples J21, J8, and J1F. Jellabia section, Gafsa Metlaoui Basin, Tunisia.

Table 2. Features of the depositional environment of fibrous clays.

| Lithological section | | Characteristics of the depositional environment |
|---|---|---|
| Stah section | Upper part | Moderate primary productivity decreases the silicic acid in the water column and $H_4SiO_4$ is less available for the formation of fibrous clay. |
| | Lower part | High primary productivity indicates that biogenic silica is abundant. Their dissolution, enhanced by a high alkalinity, produces high silicic acid concentration. |
| Jellabia section | Upper part | Despite the presence of a large Mg content which provides weathered dolomite, sepiolite cannot grow due to the lack of silicic acid. |
| | Lower part | Silicic acid is available for the formation of fibrous clay and a large Mg content generates well crystallized dolomite. |

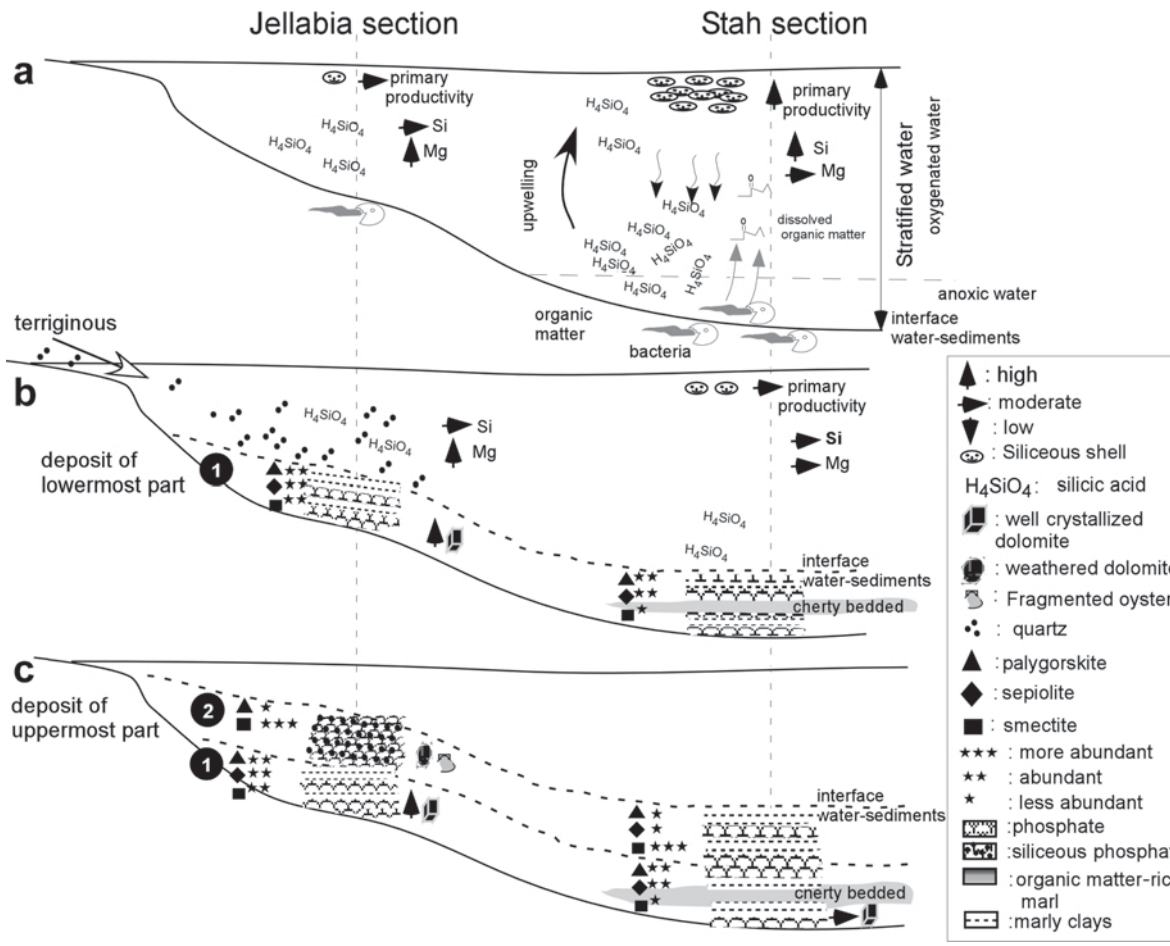


Figure 9. Simplified model of the depositional environment of clay associated with phosphatic series from the Jellabia and Stah mines. (a) Geochemical state controlling the deposition of the lowermost part. At Stah, the depositional environment was saturated by silica. Bacterial activity encourages dissolution and produces high silicic acid concentrations. At Jellabia, the depositional environment was characterized by high Mg and low Si activities, which generate well crystallized dolomite and moderate fibrous clay contents. (b) Geochemical state controlling the deposition of the uppermost part. At Stah, the low activity of Si and Mg indicates that these elements are less available for fibrous clay genesis. At Jellabia, moderate Si and high Mg activities generate weathered dolomite and small amounts of fibrous clays.

alkalinity enhanced by bacterial activity under anoxic conditions. Birsoy (2002) determined that amorphous silica in solution increases the precipitation of palygorskite-sepiolite. The small silicic-acid content in the uppermost part of the Stah section, due to the small degree of primary production, generates a small quantity of palygorskite-sepiolite.

A moderate silicic-acid content contributes to the modest amounts of palygorskite-sepiolite, whereas a large Mg content generates well crystallized dolomites (Figure 7*A*, 7*B*). Growth, *in situ*, of well crystallized dolomite also requires high alkalinity, in addition to a large Mg content (Sigg *et al.*, 1992). Analogous observations in Oligo-Miocene successions have revealed that dissolution of silica and crystallization of dolomite are contemporaneous (Bernoullia and Gunzenhauser, 2001). This condition occurs at the lowermost part of the Jellabia section where Mg from sea water is sufficient for the formation of palygorskite-sepiolite (*e.g.* Singer, 1979). In contrast, the presence of oysters within bioturbated sediments indicates a well oxygenated environment at the uppermost part of the Jellabia section.

The variation of palygorskite-sepiolite minerals in the same restricted basin, along the Stah and Jellabia sections, indicates that the vertical distribution of palygorskite-sepiolite is related to the physical-chemical conditions of sea water. According to Isphording (1973, 1984) and Chamley (1989), the genesis of fibrous clays is related to the alkalinity, Si and Mg availability, and Mg/Ca ratio. When the Mg/Ca ratio is too large, sepiolite and dolomite occurred together, as observed in the

lowermost part of the Jellabia section. The occurrence of palygorskite as a single fibrous mineral is due to its resistance to the chemical weathering process (Caillère and Hénini, 1948). The absence of sepiolite and the presence of weathered dolomite indicate that Mg is available for sepiolite formation, which could have been a major component, but this may have been mobilized or dissolved preferentially. In addition, the crystallization of palygorskite minerals may be related to the large Fe content, as confirmed by ferruginous sampled specimens. In fact, this interpretation agrees with the Fe content determined by EDX analysis observed in all samples.

The main features of the depositional environments are summarized in Table 2 and in the simplified model in Figure 9.

## CONCLUSIONS

The results obtained show that the interbedded deposits of two selected Ypresian series (Jellabia and Stah) in the Gafsa-Metlaoui basin consists of francolite, calcite, dolomite, quartz, feldspars, and a clay fraction composed of palygorskite-sepiolite associated with smectite. The trends of variation of these clay-mineral assemblages reveal that palygorskite and sepiolite are more concentrated in the lowermost part of both sections. Authigenesis of the palygorskite-sepiolite minerals can be argued from the textural evidence given by the SEM observations. Palygorskite-sepiolite appears as thin fibers and thread-like facies covering the dolomite in samples of the Jellabia section and the thin-fiber facies in silica rich environments of the Stah section. The abundance of fine fibers of palygorskite-sepiolite within cherty beds is consistent with the authigenesis of these minerals. This abundance can be related to the bacterial activity observed in cherty beds, inducing the dissolution of silica, which saturated the depositional environment by silicic acid. The availability of Mg in the depositional environment of Jellabia favored the formation of authigenic, well crystallized dolomites, especially in the lower part where the Si activity is insufficient for the significant amount of fibrous clay generated..

## ACKNOWLEDGMENTS

This work was supported by the Research Unit of the Geological Resource and Global Change (GEOGLOB: Code 03/UR/10-02), Sciences Faculty of Sfax. The authors are grateful to Prof. Zohaier Fakhfakh (USCR MEB/03) and Dr Olfa Hchicha for the SEM investigations which took place in the Physics Department.

## REFERENCES

Arfaoui, A. and Montacer, M. (2007) Geochemical characterization given by Rock-Eval parameters and *N*-alkanes distribution on Ypresian organic matter at Jebel Chaker, Tunisia. *Resource Geology*, **57.1**, 37−46.

Baioumy, H.M., Tada, R., and Gharaie, M.H.M. (2007) Geochemistry of late Cretaceous phosphorites in Egypt: Implication for their genesis and diagenesis. *Journal of African Earth Sciences*, **49**, 12−28.

Belayouni, H. (1983) Etude de la matière organique dans la série phosphatée du bassin de Gafsa Metlaoui (Tunisie). Application à la compréhension des mécanismes de la phosphatogenèse. Doc. Thesis, Tunis II University, Tunisia, 205 pp.

Bernoullia, D. and Gunzenhauser B. (2001) A dolomitized diatomite in an Oligocene−Miocene deep-sea fan succession, Gonfolite Lombarda Group, Northern Italy. *Sedimentary Geology*, **139**, 71−91.

Bidle, K.D. and Azam, F. (1999) Accelerated dissolution of diatom silica by marine bacterial assemblages. *Nature*, **397**, 508−512.

Birsoy, R. (2002) Formation of sepiolite-palygorskite and related minerals from solution. *Clays and Clay Minerals*, **50**, 736−745.

Brindley, G.W. and Brown, G. (1980) *Crystal Structures of Clay Minerals and their X-ray Identification*. Monograph **5**, Mineralogical Society, London, pp. 197−248.

Burollet, P.F. (1956) Contribution à l'étude stratigraphique de la Tunisie centrale. *Annale Mines et Géologie Tunisie*, **18**,350.

Burollet, P.F. and Oudin J.L. (1980) Paléocène et Eocène en Tunisie: Pétrole et Phosphate. *Document de Bureau de Recherches Géologiques et Minières, Orléans*, **24**, 203−216.

Caillère, S. and Hénin, S. (1948) Occurrences of sepiolite in the Lizard serpentines. *Nature*, **63**, 962.

Castany, G. (1951) Etude géologique de l'Atlas Tunisien Oriental. *Annale Mines et Géologie Tunisie*, **8**, 632 pp.

Chaâbani, F. (1995) Dynamique de la partie orientale du bassin de Gafsa au crétacé et au paléogène. Etude minéralogique et géochimique de la série phosphatée éocène (Tunisie méridionale). Doc. Thesis, Tunis II University, Tunisia, 428p.

Chahi, A. (1996) Les minéraux argileux des gisements de phosphorites des Ganntour et de stévensite du Jebel. Rhassoul (Marroc): Nouvelle données sur les relations génétiques entre les argiles 2/1 et les argiles fibreuses en condition de surface. Doc. thesis, Marrakech University, Morocco, 166 pp.

Chahi, A., Duplay, J., and Lucas, J. (1993) Analyses of palygorskites and associated clays from the Jbel Rhassoul (Morocco); chemical characteristics and origin of formation. *Clays and Clay Minerals*, **41**, 401−411.

Chamley, H. (1989) *Clay Sedimentology*. Springer Verlag, Berlin, pp. 75−94.

Daoudi, L. (2004) Palygorskite in the uppermost Cretaceous−Eocene rocks from Marrakech High Atlas, Morocco. *Journal of African Earth Sciences*, **39**, 353−358.

Disnar, J.R., Le Start, P., Farjanel, G., and Fikri, A. (1996) Organic matter sedimentation in the northeast of the Paris Basin: Consequences for the deposition of the lower Toarcien black shales. *Chemical Geology*, **131**, 15−35.

Estéoule-Choux, J. (1984) Palygorskite in the Tertiary deposits of the Armorican Massif. Pp. 75−85 in: *Palygorskite-Sepiolite: Occurrences, Genesis and Uses* (A. Singer and E. Galán, editors). Developments in Sedimentology, **37**, Elsevier, Amsterdam.

Fakhfakh, E., Hajjaji, W., Medhioub, M., Rocha, F., López-Galindo, A., Setti, M., Kooli, F., Zargouni, F., and Jamoussi, F. (2007) Effects of sand addition on production of lightweight aggregates from Tunisian smectite-rich clayey rocks. *Applied Clay Science*, **35**, 228−237.

Felhi, M. (2010) Les niveaux intercalaires de la série yprésienne du bassin Gafsa-Métlaoui: Apports de la minér-

alogie des argiles et de la géochimie de la matière organique résiduelle à la reconstitution paléoenvironnementale. PhD thesis, Sfax University, Tunisia, 184 pp.

Felhi, M., Tlili, A., Gaied, M.E., and Montacer, M. (2008a) Mineralogical study of kaolinitic clays from Sidi El Bader in the far north of Tunisia. *Applied Clay Science*, **39**, 208–217.

Felhi, M., Tlili, A., and Montacer, M. (2008b) Geochemistry, petrographic and spectroscopic studies of organic matter of clay associated kerogen of Ypresian series: Gafsa-Metlaoui phosphatic basin, Tunisia. *Resource Geology*, **59**, 428–436.

Frost, R.L., Locos, O., Ruan, H., and Kloprogge, J.T. (2001) Near-infrared and mid-infrared spectroscopic study of sepiolite and Palygorskites. *Vibrational Spectroscopy*, **27**, 1–13.

García-Romero, E., Suárez, M., Santarén, J., and Alvarez, A. (2007) Crystallochemical characterization of the palygorskite and sepiolite from the Allou Kagne deposits, Senegal. *Clays and Clay Minerals*, **55**, 606–617.

Henchiri, M. (2007) Sedimentation, depositional environment and diagenesis of Eocene biosiliceous deposits in Gafsa basin (southern Tunisia). *Journal of African Earth Sciences*, **49**, 187–200.

Henchiri, M. and Slim-Shimi, N. (2006) Silicification of sulphate evaporites and their carbonate replacements in Eocene marine sediments, Tunisia: two diagenetic trends. *Sedimentology*, **53**, 1135–1159.

Isphording, W.C. (1973) Discussion of the occurrence and origin of sedimentary palygorskite-sepiolite. *Clays and Clay Minerals*, **21,** 391–401.

Isphording, W.C. (1984) The clays of Yucatan, Mexico: a contrast in genesis. Pp. 59–73 in: *Palygorskite-Sepiolite Occurrences, Genesis and Uses* (A. Singer and E. Galán, editors). Elsevier, Amsterdam.

Jamoussi, F., Ben Aboud, A., and López Galindo, A. (2003a) Palygorskite genesis through silicate transformation in Tunisian continental Eocene deposits. *Clay Minerals*, **38**, 187–199.

Jamoussi, F., Bédir, M., Boukadi, N., Kharbachi, S., Zargouni, Z., López-Galindo, A., and Paquet, H. (2003b) Répartition des minéraux argileux et contrle tectonoeustatique dans les bassins de la marge Tunisienne. Clay mineralogical distribution and tectono-eustatic control in the Tunisian margin basins. *Compte Rendus Geoscience*, **335**, 175–183.

Jones, B.F. and Galán, E. (1988) Sepiolite and palygorskite. Pp. 631–674 in: *Hydrous Phyllosilicates (exclusive of micas)* (S.W. Bailey, editor). Mineralogical Society of America, Washington, D.C.

Krekeler, M.P.S., Guggenheim, S., and Rakovan, J. (2004) A microtexture study of palygorskite-rich sediments from the Hawthorne Formation, Southern Georgia by transmission electron microscopy and atomic force microscopy. *Clays and Clay Minerals*, **52**, 263–274.

Krekeler, M.P.S., Morton, J., Lepp, J., Tselepis, C.M., Samsonov, M., and Kearns, L.E. (2008) Mineralogical and geochemical investigations of clay-rich mine tailings from a closed phosphate mine, Bartow, Florida, USA. *Environmental Geology*, **55**, 123–147.

Lancelet, Y. (1973) Chert and silica diagenesis in sediments from the central Pacific. *Initial Reports of the Deep Sea Drilling Project*, **17**, 377–405.

Millot, G. (1970) *Geology of Clays*. Springer-Verlag, New York, 429 pp.

Muttoni, G. and Kent, D. (2007) Widespread formation of chert during the early Eocene Climate Optimum. *Palaeogeography Palaeoclimatology Palaeoecology*, **253**, 348–362.

Pletsch, T. (2001) Palaeoenvironmental implications of palygorskite clays in Eocene deep-water from the Western Central Atlantic. Pp. 308–317 in: *Western North Atlantic Paleogene and Cretaceous Palaeooceanography* (D. Kroon, R.D. Norris, and A. Klaus, editors). Special Publication, **183**, Geological Society, London.

Pluth, J.J., Smith, J.V., Pushcharovsky, D.Y., Semenov, E.I., Bram, A., Riekel, C., Weber, H.P., and Broach, R.W. (1997) Third-generation synchrotron X-ray diffraction of 6 μm crystal of raite, $\approx Na_3Mn_3Ti_{0.25}Si_8O_{20}(OH)_2.10H_2O$, opens up new chemistry and physics of low temperature minerals. *Proceedings of the National Academy of Sciences, USA*. **94**, 12263–12267.

Sassi, S. (1974) La sédimentation phosphatée au Paléocène dans le Sud et dans le Centre Ouest de la Tunisie. PhD thesis, Paris Sud Orsay University, France, 224 pp.

Schultz, L.G. (1964) Quantitative interpretation of mineralogical composition from X-ray and chemical data for the Pierre Shale. *U.S. Geological Survey Professional Paper*, vol. **391-C**. 31 pp.

Sigg, L., Stumm, W., and Behra, P. (1992) *Chimie des milieux aquatiques: chimie des eaux naturelles et des interfaces dans l 'environnement*. Masson, Paris, 391 pp.

Singer, A. (1979) Palygorskite in sediments: detrital, diagenetic or neoformed – a critical review. *Geologische Rundschau*, **68**, 996–1008.

Singer, A. (1984) Pedogenic palygorskite in the arid environment. Pp. 169–176 in: *Palygorskite-Sepiolite: Occurrences, Genesis and Uses* (A. Singer and E. Galán, editors). Developments in Sedimentology, **37**, Elsevier, Amsterdam.

Singer, A. and Norrish, K. (1974) Pedogenic palygorskite occurrences in Australia. *American Mineralogist*, **59**, 508–517.

Velde, B. (1985) *Clay Minerals – A Physico-chemical Explanation of their Occurrences*. Elsevier, Amsterdam, pp. 225–256.

Visse, L. (1952) Genèse des gîtes phosphatée du Sud-Est Algéro-Tunisien. *XXXème Congrès de Géologie, Algerie*, **1**, 27–53.

Weaver, C.E. and Beck, K.C., editors (1977) Miocene of the S.E. United States: A model for chemical sedimentation in peri-marine environment. Developments in Sedimentology, **22**. Elsevier, Amsterdam, pp. 225–256.

Yalcin, H. and Bozkaya, O. (1995) Sepiolite-palygorskite from the Hekimhan region (Turkey). *Clays and Clay Minerals*, **43**, 705–717.

Zaaboub, N., Abdeljaouad, S., and López Galindo, A. (2005) Origin of fibrous clays in Tunisia Paleogene continental deposits. *Journal of African Earth Sciences*, **43**, 491–504.

(*Received 19 May 2009; revised 27 May 2010; Ms. 317; A.E. H. Stanjek*)